Hindawi
Advances in Civil Engineering
Volume 2018, Article ID 3138759, 7 pages
https://doi.org/10.1155/2018/3138759

Research Article

Flexural Properties of ECC-Concrete Composite Beam

Yanhua Guan, Huaqiang Yuan, Zhi Ge, Yongjie Huang, Shuai Li, and Renjuan Sun

Department of Transportation Engineering, School of Civil Engineering, Shandong University, Jinan 250061, China

Correspondence should be addressed to Zhi Ge; zhige@sdu.edu.cn

Received 27 October 2017; Accepted 12 December 2017; Published 4 March 2018

Academic Editor: Peng Zhang

Rebar corrosion-induced durability issue is a major concern for bridges. The ECC cover was employed to prevent the intrusion of the corrosive agent. This paper studied the flexural behavior of ECC-concrete composite beam. The effects of bonding at the interface and fiber mesh reinforcement on the flexural properties and cracking pattern were investigated. The strain distribution and midspan deflection were evaluated. Test results show that the bonded composite beam had a higher loading capacity. But the unbonded composite beam showed better postcrack energy absorption capacity with higher midspan deflection. The fiber mesh reinforcement could further improve the flexural properties regardless of the bonding condition. The strain at the bottom of the unbonded beam was much smaller than that of the bonded beam. The penetrated cracks were observed at the ECC layer of the bonded composited beam.

1. Introduction

The long-term durability of bridges has become a major concern, especially for bridges exposed to aggressive environmental conditions. In 2015, about 79.6 thousand bridges, which is 10.2% of the total bridges, were classified as dangerous in China [1]. The main cause of bridge deterioration is the corrosion of reinforcing steel, which results in reduced service life [2] or even collapse. To prevent steel corrosion, a certain thickness of concrete cover is designed for reinforced concrete structures. However, in practice, concrete cover will definitely crack due to mechanical and environmental loading, low tensile strength of concrete, and so on, thereby creating a fast entry path for corrosive agents and causing corrosion [3]. Therefore, one of the key points of prolonging bridge service life is to prevent cracking and reduce the permeability of the concrete cover.

Engineered cementations composite (ECC) developed based on micromechanics has a high ductility and crack control capacity (crack widths less than 100 μm) even at large deformation [4, 5]. Besides the excellent mechanical properties, a large amount of researches show that ECC has much higher durability than that of normal concrete [6–8]. Researches indicate that even strained in tension up to 3%, the permeability and chloride ion diffusivity of ECC were similar to that of uncracked concrete [9, 10]. These unique properties make ECC very suitable as concrete cover for bridges under aggressive environments [11]. Researches have been carried out to investigate the mechanical properties of the reinforced ECC-concrete composite beam [12–19]. Compared to normal reinforced concrete, properties, including load-carrying capacity, deformability, crack controlling ability, and fatigue, of beam with ECC layer were improved significantly. The ultimate strength and deflection improvement in composite beams are mainly dependent on the tensile and compressive ductility of the matrix [20].

In most of the current studies, the ECC layer was fully bonded with the normal concrete. Therefore, these two layers could deform together and increase the load-carrying capacity. However, large cracks developed at the concrete could cause localized cracking in the ECC layer [15, 19]. Some cracks could still penetrate through the ECC layer, resulting in an entry path for corrosive agents. In this situation, the high ductility and durability of the ECC could not be fully utilized. In order to prevent the penetrated crack in the ECC cover, the unbound composite beam is proposed in this paper. A plastic sheet was placed at the interface of normal concrete and ECC to break the bond. Large strain caused by the cracking in the normal concrete will be distributed across the entire ECC layer, avoiding the strain

Table 1: The main chemical components of cement.

Components	CaO	SiO_2	Al_2O_3	MgO	P_2O_5	K_2O	SO_3	Na_2O
Content (%)	75.4	21.9	1.3	1.3	0.03	2.7	2.0	0.07

Table 2: Characteristics of PVA fiber.

Diameter (μm)	Length (mm)	Nominal strength (MPa)	Young's modulus (GPa)	Elongation (%)	Density (kg/m^3)
39	12	1620	42.8	7.0	1300

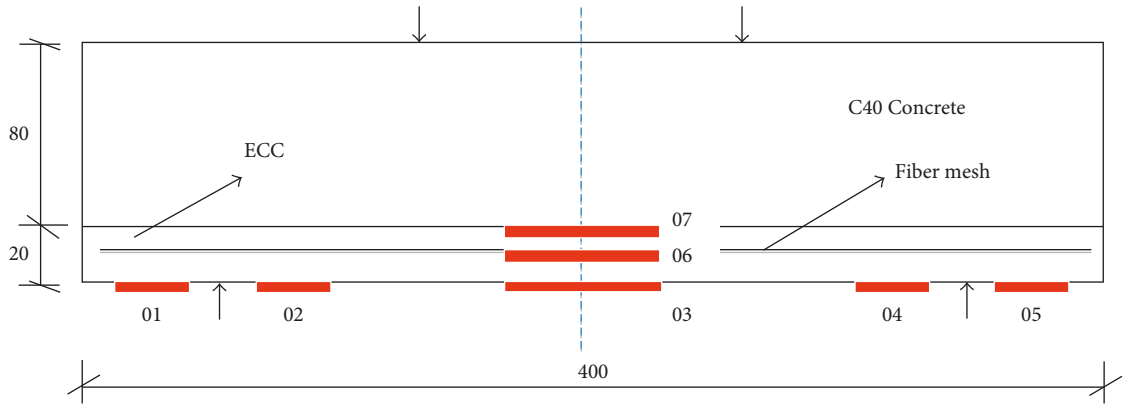

Figure 1: Configurations of strain-testing points of the composite beam.

concentration. A fiber mesh reinforcement was also placed in the middle of the ECC layer to further increase its strength and ductility. In this paper, the effects of bonding and reinforcement of ECC on the flexural properties of the composite beam were investigated.

2. Materials and Methods

2.1. Materials. The cement used was ordinary 42.5# Portland cement with a 28-day compressive strength of 42.5 N/mm^2. The main chemical components of cement are provided in Table 1. The class F fly ash containing 3.88% CaO from Jinan, Shandong province, was adopted. The characteristics of used PVA fiber are listed in Table 2. The high-range water reducer (HRWRA) and viscosity-modifying agent (VMA) were employed simultaneously to obtain the proper workability. Based on the previous study, the water to cement ratio of 0.32, fly ash to cement ratio of 1.2, silica sand to cement ratio of 0.8, and 2% (by volume) of fiber were adopted for ECC mix. The concrete with the compressive strength of 40 MPa (C40) was used for the composite beam.

2.2. Experiment Design. The $100 \times 100 \times 400$ mm composite beam with a 20 mm ECC layer at the bottom was casted for the study. Two types of the ECC layer were considered. One is the pure ECC layer and the other is the reinforced ECC layer with fiber mesh reinforcement in the middle. Two interface bonding conditions, fully bonded and unbonded, between normal concrete and ECC layer were designed. Therefore, four different types of ECC-concrete composite beams were studied. During the four-point bending testing, the strain at different locations and midspan deflection was monitored. The configurations of the strain gauges are shown in Figure 1.

2.3. Specimen Preparation. The C40 concrete was first mixed according to GB/T 50081-2002 [21] and casted in the mold. The reinforcing steel was then embedded into the concrete. After cured for 24 hours, the ECC was mixed and casted on top of the normal concrete. The beam was then cured in the standard curing room with $20 \pm 2^{\circ}$C temperature and 95% humidity for 28 days. For the unbonded composite beam, a plastic sheet was place on top of the normal concrete before placing ECC to prevent the bonding between ECC and normal concrete. The ECC layer was anchored at both ends. For the reinforced ECC layer, the fiber mesh was placed at the middle of the ECC layer before casting ECC.

2.4. Testing Methods. The uniaxial tensile and four-point bending tests were conducted to evaluate the properties of ECC. The 15 mm $\times$ 50 mm $\times$ 350 mm specimen was used for both tests. The LVDT displacement sensors were employed to measure displacement. The universal testing machine (WDW-100E) was used for loading. The loading rates were 0.1 mm/min and 0.5 mm/min for direct tensile and four-point bending tests, respectively. The testing setups are shown in Figure 2. For the composite beam, the four-point bending test was carried out by using the microcomputer-controlled electronic universal testing machine under displacement control at the rate of 0.5 mm/min until its failure. The strain at different locations was collected by DH3818-4 strain acquisition box. The midspan deflection was measured by LVDT.

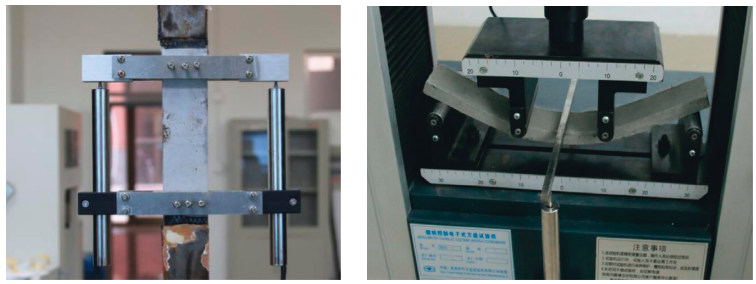

(a) (b)

Figure 2: Test setups for direct tensile and four-point bending tests of ECC. (a) Uniaxial tensile test. (b) Four-point bending test.

3. Results and Discussion

3.1. Properties of ECC Material. Figures 3 and 4 show that, under both uniaxial tensile and flexural loading, ECC exhibits strain hardening behavior. The first cracking strength was 2.9 MPa. After the first cracking, the load continued to increase without fracture localization. Sequentially, more cracks developed, resulting in the inelastic strain at increasing stress. The ultimate tensile strength and tensile strain capacity were 4.4 MPa and 4.5%, respectively.

The flexural behavior was similar to that under uniaxial tensile loading (Figure 4). The four-point bending test could be used as an indirect evaluation method for the strain-hardening properties of ECC [22]. The midspan deflection reached 20.5 mm at failure. The first cracking strength and flexural strength were 7.7 and 14.7 MPa, respectively, which were much higher than those of normal concrete.

The typical microcracking patterns of specimen under uniaxial tensile and flexural loading are shown in Figure 5. As observed in the figures, microcracks with very tight crack width were uniformly distributed with an average spacing less than 1 mm. The cracking pattern also indicated that the ECC had a very good strain-hardening property.

3.2. Flexural Behavior of Composite Beam. As shown in Figure 6, both composite beams show elastic and plastic behavior under the flexural loading. At the beginning, the midspan deflection increased linearly with the flexural loading. At the end of the linear portion there was a force drop, it could be caused by the cracking of ECC and yielding of reinforcement steel. After that, more deflection occurs. Figure 6 also indicates that, regardless of whether the fiber mesh was embedded in the ECC layer, the type of bonding between the concrete and ECC layer had significant effect on both the flexural loading capacity and midspan deflection. Since the ECC had high tensile strength and ductility, it will carry the tensile strength together with the steel reinforcement after concrete cracks, resulting in higher strength. This trend is consistent with other research works [15, 18, 19]. Differently, the unbonded composite beam showed a great postcrack energy absorption capacity due to the deformation of the ECC layer. The unbonded ECC cover could be treated as an external strengthening reinforcement. Since slip at the interface was allowed, the longitudinal strain was distributed across the ECC cover, thereby, allowing higher deflection.

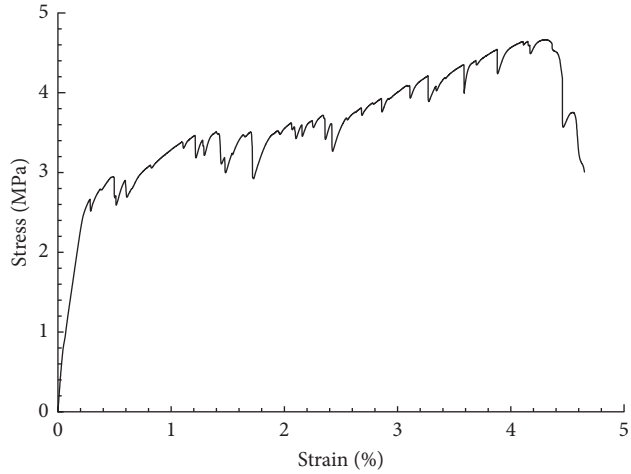

Figure 3: Uniaxial tensile stress-strain curve of ECC.

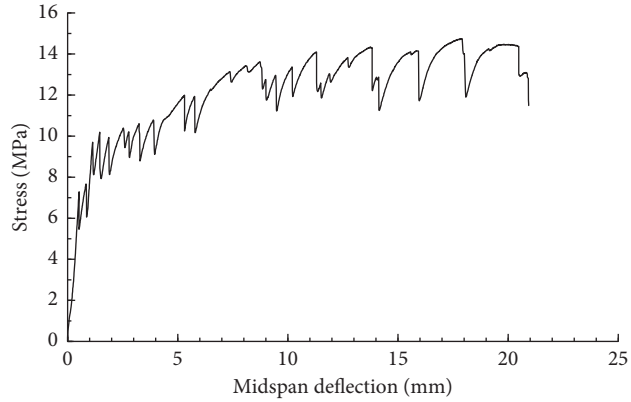

Figure 4: Midspan deflection under flexural loading.

This finding is similar to Kamada and Li's research. They also found that the interface property could affect the flexural behavior of the composite beam. The smooth surface specimen was able to redistribute the load and utilize more materials than rough surface specimens. Therefore, the deflection of the smooth beam was larger than that of the rough beam [23].

Placing a fiber mesh in the middle of the ECC layer could further increase its tensile strength and ductility, which in turn increased the loading capacity and midspan deflection

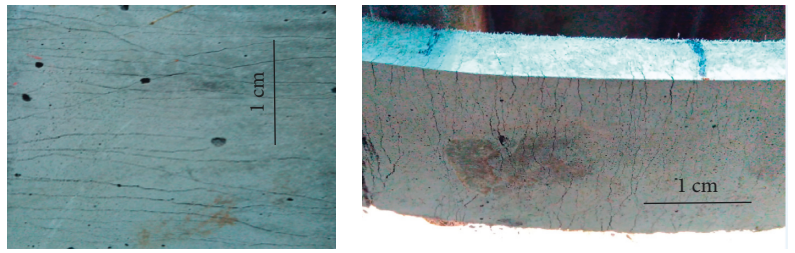

Figure 5: Multiple microcracking patterns under different loading. (a) Crack under uniaxial tensile loading. (b) Crack under flexural loading.

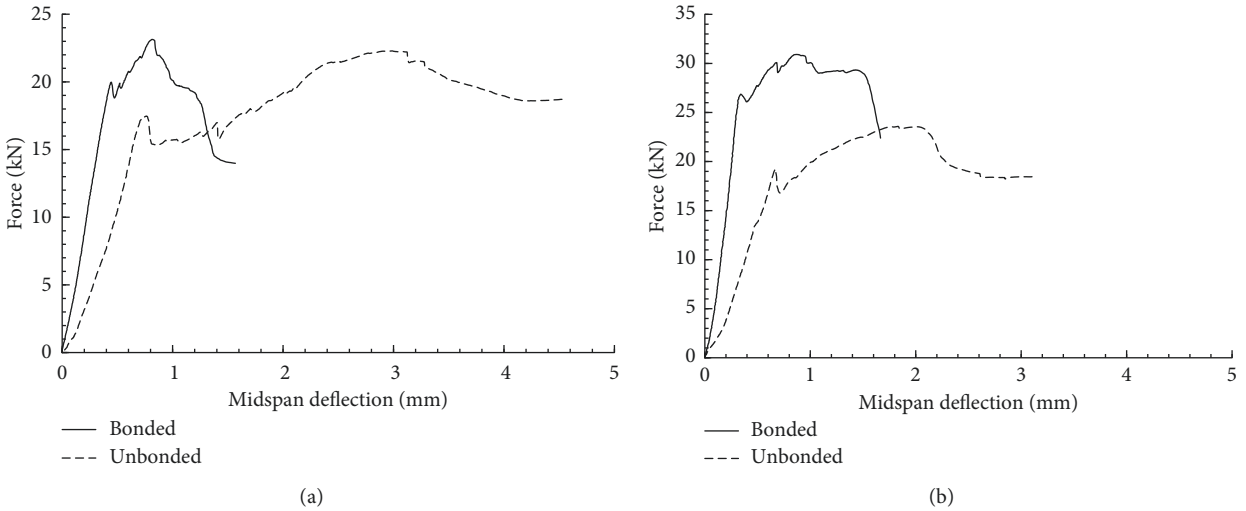

Figure 6: Effect of bonding conditions on composite beam behavior. (a) Without fiber mesh. (b) With fiber mesh.

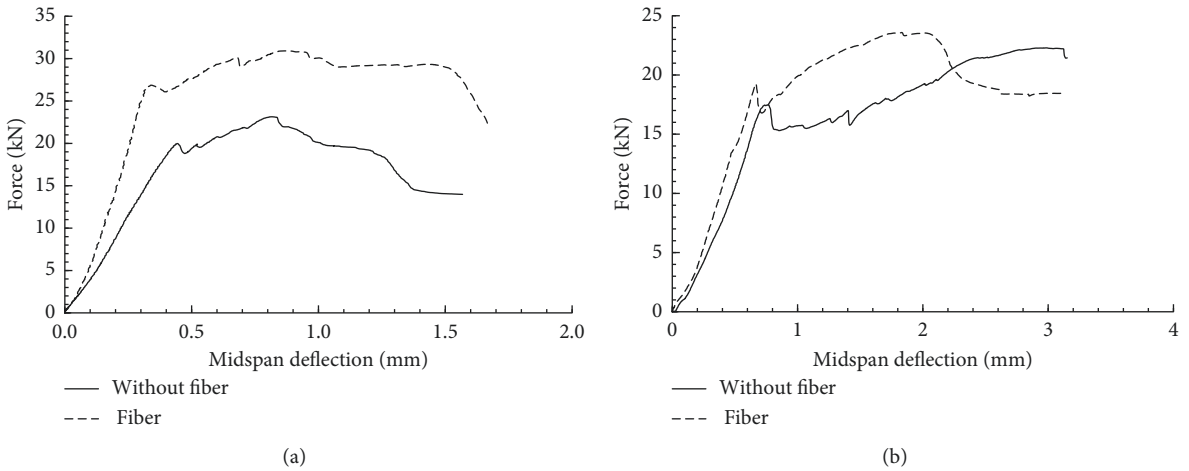

Figure 7: Effect of fiber mesh on composite beam behavior. (a) Fully bonded. (b) Unbonded.

at failure (Figure 7). This effect is more prominent for the bonded composite beam. The increments were 50% and 70% for the loading capacity and midspan deflection at failure, respectively. The midspan deflections were 2.1 and 3.0 mm for the unbonded beam with and without fiber mesh reinforcement, respectively.

3.3. Load-Strain Pattern of Composite Beams. The load versus strain at different locations of the bottom is plotted in Figure 8. These two types of beam possessed totally different patterns. For the unbonded composite beam, the tensile strains at points 1 and 2 were negligible due to very small stress and bending moment. The major strain occurred at the

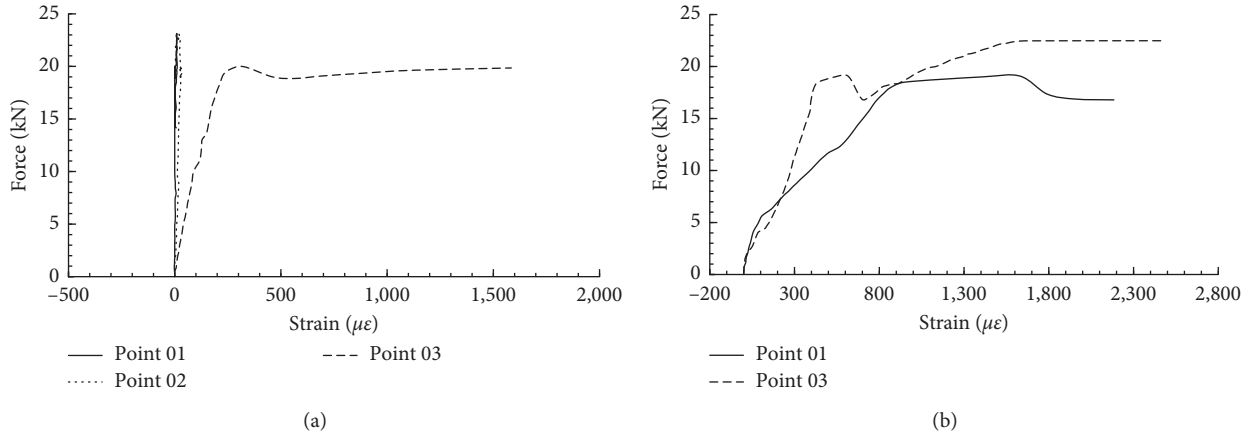

Figure 8: Strain at different locations of beam bottom. (a) Fully bonded. (b) Unbonded.

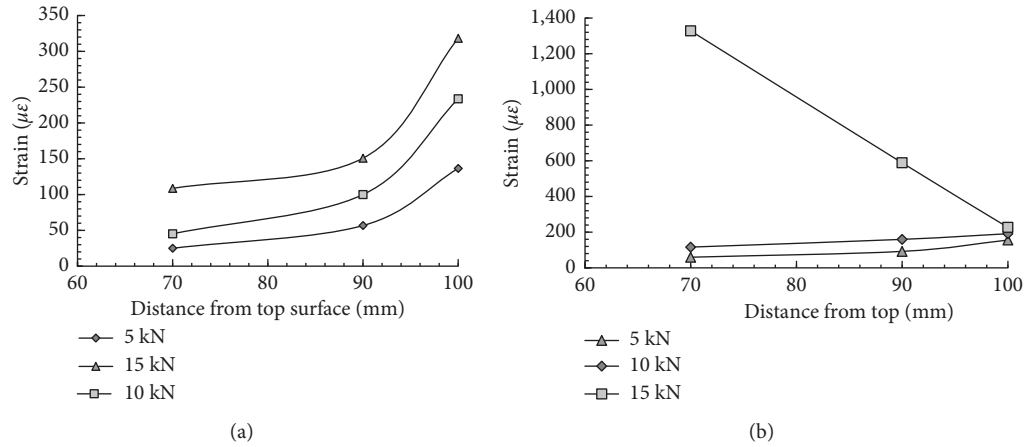

Figure 9: Strain distribution at the midspan section. (a) Fully bonded. (b) Unbonded.

middle of the span. Differently, the strain at point 1 of the unbonded composite beam was close to that of point 3. Because of the slip at the interface, there was limited shear resistance. The load carried by the ECC layer would pass to the anchors at both ends. In this case, all ECC layers were under tension and had similar tensile strain at the longitudinal direction. This means that under the same deflection, the ECC layer of the unbonded composite beam had smaller strain and lower risk of cracking than that of the bonded beam.

Figure 9 shows the strain distribution at the midspan section of the composite beam. Figure 9(a) indicates that the bonding between the ECC and normal concrete was strong and no slip occurred. The trend is similar to the current research work [16]. But for the unbonded composite beam, the strain of the ECC layer increased slowly with the load. When loaded at 15 kN, the strain was 1328 $\mu\varepsilon$ at point 7. But the bottom strain at point 3 was only 227 $\mu\varepsilon$. The high-strain value at point 7 was caused by the cracking of normal concrete. Figure 9 also indicates that under the same loading the strain at the bottom of the unbonded beam was much smaller than that of the bonded beam. This further proves that the ECC layer of the unbonded composite beam had lower risks of cracking, making the ECC suitable as concrete cover for corrosion resistance.

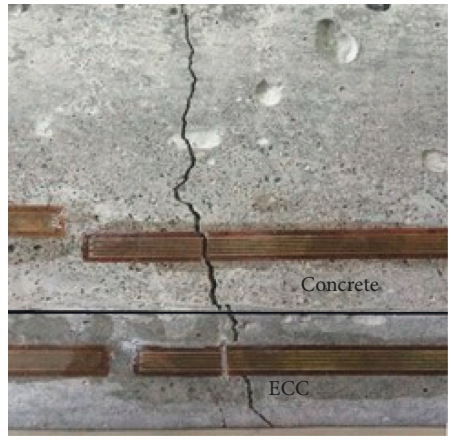

Figure 10: Cracking pattern of the bonded composite beam.

3.4. Cracking Pattern of the Beams. Figures 10 and 11 show the cracking pattern of different beams. Even though ECC had very high ductility, localized cracks still occurred at the ECC cover of the bonded composite beam (Figure 10) due to the concentrated strain. A major crack right beneath the crack of the normal concrete penetrated through the

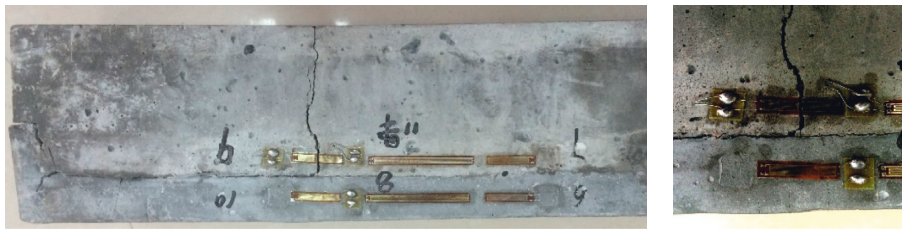

(a) (b)

Figure 11: Cracking pattern of the unbonded composite beam.

ECC cover. Although the ECC cover improved the beam's mechanical performance, there were still risks of corrosion of the rebar inside the beam and reduction of service life of the bonded composite beam. Differently, there were no cracks penetrating through the ECC cover for the unbonded composite beam. Also, the crack's width at the ECC cover was limited due to the high crack control capacity. The average crack widths at failure were 115 and 98 μm for the unbonded composite beam without and with fiber reinforcements, respectively. Therefore, even though there were cracks at the ECC cover, the permeability would be limited due to very small crack width, resulting in high durability. Figure 11 also shows cracking at the left end of the ECC layer. Since the ECC layer could be treated as the external reinforcement of the unbonded composite beam, the force provided by the ECC layer is transferred to the normal concrete in the compression mode through end anchors, resulting in tensile stresses in the end anchors. If the stress is large enough, it will lead to cracking and failure of the anchor.

4. Conclusions

This paper studied the effects of bonding and fiber mesh reinforcement on the flexural properties and cracking pattern of the composite beams. The following findings and conclusions can be drawn:

(1) ECC exhibits strain-hardening behavior. The first cracking strength, ultimate tensile strength, and tensile strain capacity were 2.9 MPa, 4.4 MPa, and 4.5%, respectively

(2) The bonded composite beam had a higher loading capacity. But the unbonded composite beam showed a better postcrack energy absorption capacity. The fiber mesh reinforcement could further improve the flexural properties, regardless of the bonding condition

(3) The unbonded ECC layer had the ability to distribute the strain across the beam. Under the same loading, the strain at the bottom of the unbonded beam was much smaller than that of the bonded beam

(4) Localized cracking could penetrate through the ECC cover of the bonded composite beam. The average cracking widths were controlled at 115 and 98 μm for unbonded composite beam without and with fiber reinforcements.

The results of this study indicate that the unbonded ECC cover is more effective in terms of controlling the cracking and preventing the corrosion-induced damage. Therefore, the unbonded composite beam could be used for bridges under aggressive environments to enhancing its service life. However, further study is needed to quantify the effect of the bonding on the beam behavior and to explore the durability of the composite beam.

Conflicts of Interest

The authors declare that they have no conflicts of interest.

Acknowledgments

The financial support is provided by Tai'an Tong Da Investment Co., Ltd., Ji Nan Tong Da Highway Engineering Co., Ltd., and the Natural Science Foundation of China of Shandong (ZR2016EEM03). Sincere acknowledgements are also given to Nan Gao, Changjin Tian, and Yida Wang for their great assistance.

References

[1] Q. S. Wang, "The supplement of evaluation system of the current-existed bridges," M.S. thesis, Chongqing Jiaotong University, Chongqing, China, 2016.

[2] M. D. Lepech, "A paradigm for integrated structures and materials design for sustainable transportation infrastructure," Ph.D. thesis, University of Michigan, Ann Arbor, MI, USA, 2006.

[3] M. Li, R. Ranade, L. Kan, and V. C. Li, "On improving the infrastructure service life using ECC to mitigate rebar corrosion," in *Proceedings of the 2nd International Symposium on Service Life Design for Infrastructure*, Delft, Netherlands, October 2010.

[4] V. C. Li, H. Stang, and H. Krenchel, "Micromechanics of crack bridging in fiber reinforced concrete," *Materials and Structures*, vol. 26, no. 8, pp. 486–494, 1993.

[5] V. C. Li, Y. Wang, and S. Backer, "A micromechanical model of tension-softening and bridging toughening of short random fiber reinforced brittle matrix composites," *Journal of the Mechanics and Physics of Solids*, vol. 39, no. 5, pp. 607–625, 1991.

[6] H. Z. Liu, Q. Zhang, V. Li, H. Z. Su, and C. S. Gu, "Durability study on engineered cementitious composites (ECC) under sulfate and chloride environment," *Construction and Building Materials*, vol. 133, pp. 171–181, 2017.

[7] K. Turk and S. Demirhan, "Effect of limestone powder on the rheological, mechanical and durability properties of ECC," *European Journal of Environmental and Civil Engineering*, vol. 21, no. 9, pp. 1151–1170, 2017.

[8] V. C. Li, G. Fischer, Y. Kim et al., "Durable link slabs for jointless bridge decks based on strain-hardening cementitious composites," Report RC-1438, Michigan Department of Transportation, Cadillac, MI, USA, 2003.
[9] M. D. Lepech and V. C. Li, "Water permeability of cracked cementitious composites," in *Proceedings of the Compendium of Papers, ICF11*, Turin, Italy, March 2005.
[10] M. Sahamaran, M. Li, and V. C. Li, "Transport properties of engineered cementitious composites under chloride exposure," *ACI Materials Journal*, vol. 104, no. 6, pp. 604–611, 2007.
[11] V. C. Li, "On engineered cementitious composites (ECC)–a review of the material and its applications," *Journal of Advanced Concrete Technology*, vol. 1, no. 3, pp. 215–230, 2003.
[12] M. Maalej and V. C. Li, "Introduction of strain hardening engineered cementitious composites in design of reinforced concrete flexural members for improved durability," *ACI Structural Journal*, vol. 92, no. 2, pp. 167–176, 1995.
[13] M. Maalej and V. C. Li, "Flexural strength of fiber cementitious composites," *Journal of Materials in Civil Engineering*, vol. 6, no. 3, pp. 390–406, 1994.
[14] J. M. Cai, J. L. Pan, and X. M. Zhou, "Flexural behavior of basalt FRP reinforced ECC and concrete beams," *Construction and Building Materials*, vol. 142, pp. 423–430, 2017.
[15] M. I. Khan and W. Abbass, "Flexural behavior of high-strength concrete beams reinforced with a strain hardening cement-based composite layer," *Construction and Building Materials*, vol. 125, pp. 927–935, 2016.
[16] Z. Z. Yu, W. W. Wen, and J. C. Brigham, "Flexural behaviour of reinforced concrete beams strengthened with a composite reinforcement layer: BFRP grid and ECC," *Construction and Building Materials*, vol. 115, pp. 424–443, 2016.
[17] Y. Yan, Y. Xu, X. Wang, and J. L. Pan, "Flexural behaviors of double-reinforced ECC beams," *Journal of Southeast University*, vol. 29, no. 1, pp. 66–72, 2013.
[18] S. B. Singh and M. V. R. Sivasubramanian, "Flexural response of ECC strengthened reinforced concrete beams," *Indian Concrete Journal*, vol. 87, no. 7, pp. 35–44, 2013.
[19] M. Hussein, M. Kunieda, and H. Nakmura, "Strength and ductility of RC beams strengthened with steel-reinforced strain hardening cementitious composites," *Cement and Concrete Composite*, vol. 34, no. 9, pp. 1061–1066, 2012.
[20] F. Yuan, J. L. Pan, and Y. F. Wu, "Numerical study on flexural behaviors of steel reinforced engineered cementitious composite (ECC) and ECC/concrete composite beams," *Science China Technological Sciences*, vol. 57, no. 3, pp. 637–645, 2014.
[21] GB/T 50081-2002, *Standard for Test Method of Mechanical Properties on Ordinary Concrete*.
[22] X. R. Cai and S. L. Xu, "Study on corresponding relationships between flexural load-deformation hardening curves and tensile stress-strain hardening curves of UHTCC," *Engineering Mechanics*, vol. 27, no. 1, pp. 8–16, 2010.
[23] T. Kamada and V. C. Li, "The effects of surface preparation on the fracture behavior of ECC/concrete repair system," *Cement and Concrete Composite*, vol. 22, no. 6, pp. 423–431, 2000.